Monthly Notices
of the
ROYAL ASTRONOMICAL SOCIETY

MNRAS **461,** L117–L121 (2016)
Advance Access publication 2016 May 16

doi:10.1093/mnrasl/slw099

The disappearance of the helium-giant progenitor of the Type Ib supernova iPTF13bvn and constraints on its companion

J. J. Eldridge[1]★ and J. R. Maund[2]★

[1]*Department of Physics, University of Auckland, Private Bag 92019, Auckland, New Zealand*
[2]*Department of Physics and Astronomy, University of Sheffield, Hicks Building, Hounsfield Road, Sheffield S3 7RH, UK*

Accepted 2016 May 12. Received 2016 May 9; in original form 2016 March 20

ABSTRACT

We report and discuss post-explosion observations of supernova iPTF13bvn. We find that the brightness of the supernova (SN) at +740 d is below the level of the pre-explosion source and thus confirm that the progenitor has exploded. We estimate that the late-time brightness is still dominated by the SN, which constrains the magnitude and thus mass of a possible companion star to below approximately 10 $M_\odot$. In turn, this implies that the progenitor's initial mass is constrained to a narrow range between 10 and 12 $M_\odot$. The progenitor of iPTF13bvn would have been a helium giant rather than a Wolf–Rayet star. In addition, we suggest that sufficiently deep observations acquired in 2016 would now stand a chance to directly observe the companion star.

Key words: binaries: general – stars: evolution – stars: massive – supernovae: general – supernovae: individual: iPTF13bvn.

1 INTRODUCTION

Cao et al. (2013) reported the detection of a possible progenitor for the Type Ib supernova (SN) iPTF13bvn in pre-explosion observations of NGC 5806. Due to this being the first such detected candidate for a hydrogen-free Type Ib/c SN progenitor, the pre-explosion observations were reanalysed by a number of authors including Groh, Georgy & Ekström (2013), Fremling et al. (2014) and Bersten et al. (2014). The latter study by Bersten et al. suggested that the progenitor was probably a binary system composed of two relatively low-mass stars, in which an interaction between the two components was responsible for removing hydrogen from the progenitor. This model was consistent with the prediction by Yoon et al. (2012) that it would be easier to detect these helium-giant systems than more massive Wolf–Rayet (WR) progenitor stars. Conversely, Groh et al. (2013) suggested that a WR star progenitor could still be possible if the progenitor had been rapidly rotating on the main sequence.

In Eldridge et al. (2015), it was shown that the initial magnitudes reported by Cao et al. (2013) were in error and the pre-explosion source was brighter. The new photometry of the pre-explosion source was compared to a large range of interacting binary models from the Binary Population and Spectral Synthesis code (BPASS).[1] A number of models were found, with initial masses from 9 to 20 $M_\odot$, that matched the source in the pre-explosion images as well as the supplementary constraints from modelling the SN, as discussed by Fremling et al. (2014) and Bersten et al. (2014). In these results, a standard non-rotating single-star model was strongly disfavoured as a possible progenitor.

Here, we report on the detection of the SN in late-time observations at magnitudes, finding it to be fainter than the pre-explosion source and faint enough that the mass of the companion star can be constrained. This constraint again strongly disfavours a WR star as the progenitor of the SN and the best model progenitors are helium giants with an initial mass of approximately 10–12 $M_\odot$.

2 ON THE LATE-TIME SN BRIGHTNESS

The pre-explosion observations of iPTF13bvn, in which the progenitor candidate was identified were previously presented by Cao et al. (2013) and Eldridge et al. (2015). The brightness of the progenitor object was found to be $F435W = 25.80 \pm 0.12$, $F555W = 25.80 \pm 0.11$, and $F814W = 25.88 \pm 0.24$ mag.

Late-time observations of the site of iPTF13bvn were acquired with the Wide Field Camera 3 (WFC3) Ultraviolet–Visible channel (UVIS) on 2015 June 26 (approximately 740 d post-explosion; Cao et al. 2013). The observations, which were immediately made public, were acquired as part of programme GO-13684 (P.I. S. Van Dyk). The observations were composed of two sequences of exposures of 2 × 2860 s and 2860 + 2750 s using the *F*438*W* and *F*555*W* filters, respectively. The constituent exposures were combined using the ASTRODRIZZLE package, running in the PYRAF environment.[2] The position of the SN was identified on the late-time images through comparison with post-explosion WFC3 UVIS observations of iPTF13bvn acquired on 2013 September 2 as part of programme GO-12888 (P.I. S. Van Dyk). A geometric transformation between the post-explosion and late-time images was calculated using 35 common stars, with resulting uncertainty on the

★ E-mail: j.eldridge@auckland.ac.nz (JJE); j.maund@sheffield.ac.uk (JRM)
[1] http://bpass.auckland.ac.nz

[2] STSDAS and PYRAF are products of the Space Telescope Science Institute, which is operated by AURA for NASA.

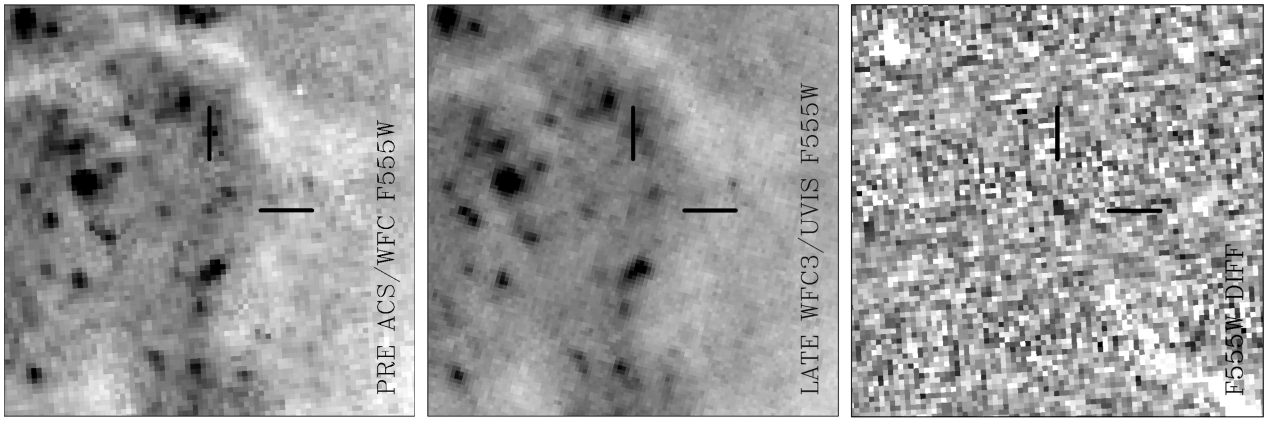

Figure 1. Pre-explosion and late-time (left and centre) *HST* observations of the site of iPTF13bvn, acquired with the ACS/WFC and WFC3/UVIS. The SN position on all frames is indicated by the cross-hairs. On the right is shown a difference image, calculated between the pre-explosion and late-time *F555W* observations using the ISIS image subtraction package (Alard & Lupton 1998; Alard 2000).

SN position in the late-time images of 0.36 px (or 14 mas). A source is recovered on the late-time images within 1σ from the transformed SN position. Photometry of the late-time images was conducted using the DOLPHOT package[3] (Dolphin 2000) and the brightness of the source at the SN position was measured to be $m_{F438W} = 26.48 \pm 0.08$ and $m_{F555W} = 26.33 \pm 0.05$ mag. We note that the sharpness parameter, measured by DOLPHOT, was found to be -0.430 and -0.560 in the *F438W* and *F555W* images, respectively. These values are just outside the range of sharpness values expected for point-like sources, that may suggest that the recovered source is slightly extended. The SN position on the pre-explosion and late-time *F555W* images is shown on Fig. 1.

The post-explosion source is 0.68 and 0.53 mag fainter than the pre-explosion source in the *F438W* and *F555W* observations; although we note that the pre-explosion and late-time *B*-band observations were acquired with slightly different filters. The brightness of the post-explosion source is below the level of the pre-explosion source, confirming that the pre-explosion progenitor candidate was the progenitor which has now disappeared.

In Eldridge et al. (2015), we derived a range of absolute magnitudes in each filter due to the uncertainty in the extinction towards the pre-explosion source. We reuse the same values here, we adopt a distance of 22.5 ± 2.4 Mpc, $\mu = 31.76 \pm 0.36$ mag and assume that the reddening is between ($E(B-V) = 0.045$) and 0.17 ± 0.03 mag. We note that there is an updated distance from Tully et al. (2013), who report a distance modulus of $\mu = 32.14 \pm 0.20$. To allow for this extra uncertainty, we use this greater distance to calculate the upper limits and the shorter distance for the lower limits. For the *F435W* and *F555W* observations, these were between $-6.15 \leq M_{F435W} \leq -6.89$ and $-6.1 \leq M_{F555W} \leq -6.71$. Here, we find that the range of absolute magnitudes for the post-explosion source are between $-5.47 \leq M_{F435W} \leq -6.21$ and $-5.57 \leq M_{F555W} \leq -6.18$. With these magnitudes below the previous pre-explosion source, we know that source was the progenitor which has now disappeared. We find that using the distance does not significantly alter the nature of our fit but does decrease the mean metallicity slightly.

To estimate whether this source could still be the SN or another object, we have compared our photometry with earlier *B*- and *V*-band observations of Srivastav, Anupama & Sahu (2014) and Kuncarayakti et al. (2015). We list the known *B*- and *V*-band magnitudes in Table 1. We then use the last observed magnitudes and the decay rate from Kuncarayakti et al. (2015) to predict what the expected magnitudes should be on the date of the *Hubble Space Telescope* (*HST*) observations. The *B*/*F438W* magnitudes are quite close and we thus can only assume that this flux arises from the SN itself. We see however that the *V*/*F555W* magnitudes are quite different with the observed flux being significantly brighter than expected from the previous behaviour of the light curve. We note, however, that Kuncarayakti et al. (2015) measured the *V*-band decay rate to be 1.55 mag per 100 d, which is significantly higher than the decay rates of 1.13 and 1.32 measured for the *B*- and *R*-band photometry.

Table 1. Photometry of iPTF13bvn.

Date	Phase[a] (d)	$m(B/F438W)$ (mag)	$m(V/F555W)$ (mag)
2013/08/06	53.93	18.2	–
2013/09/10	88.84	–	17.8
2014/04/18	324	21.1	21.2
Expected	740	26.0	28.0
2015/06/26	740	26.5	26.3
Expected	1001	29.6	29.7

Note. [a]with respect to the explosion date 2013 June 15.67; Cao et al. (2013)

To gain some insight into the possible late-time behaviour of iPTF13bvn, we have also compared the behaviour to SN 2011dh, as described by Ergon et al. (2015) because Fremling et al. (in preperation) show that the evolution of these two SNe are very similar. The light curve of 2011dh begins to flatten at ≈450 d. Other authors have also shown evidence that this is also true for iPTF13bvn (Folatelli et al. 2016; Fremling et al., in preperation).

At 700 d, the $B-V$ colour of 2011dh is very similar to the value we observed for iPTF13bvn. This gives us some confidence that we are indeed observing the SN at these late times. Predicting the emission of an SN at such a late time is difficult. As discussed by Ergon et al. (2015), at 700 d, there can be many contributions driving the light curve. For example, positrons emitted in the ^{56}Co decay can deposit more energy than the γ-rays from the same decay. Therefore, accurate prediction of late-time behaviour is possible, but there is a certain amount of uncertainty.

If we assume that long-term evolution should be mostly similar and that it becomes shallower over a longer time, we can assume

[3] http://americano.dolphinsim.com/dolphot/

that the decay rates between the different filters should be more similar. Using our photometry and comparing them to the latest magnitudes reported by Srivastav et al. (2014), we find decay rates of 1.20 and 1.30. The similarity between the decay rates, as well as to 2011dh, suggest that the source detected is, in fact, the SN and not a companion star.

3 NUMERICAL METHOD

In this Letter, we use the latest BPASS v2.0 models rather than the previous v1.1 as used in Eldridge et al. (2013, 2015). These models are almost identical in construction as described in detail in Eldridge, Izzard & Tout (2008); however, there are more initial masses, more initial separations, more masses for each companion star, and a wider range of metallicities. Full details of v2.0 will be described in Eldridge et al. (in preperation). They have already been used in a few studies including Stanway, Eldridge & Becker (2016) and Wofford et al. (2016), and have been found to match previous results well. Here, we use these models and compare them to the progenitor candidate in a similar method to Eldridge et al. (2015), with an extended grid of stellar models. The key difference to the analysis of Eldridge et al. is that we can now use the late-time *HST* photometry of the source at the position of iPTF13bvn to constrain the brightness of a possible companion.

We show the details of the resulting matching models in Fig. 2, in which the locations of the primary and companion stars are shown on the Hertzsprung–Russell (HR) diagram. In Fig. 3, we compare the pre-explosion and late-time magnitudes to the pre- and post-explosion magnitudes expected from our stellar models. We also provide the mean parameters for the progenitor and companion calculated from all the models that fit the observations in Table 2.

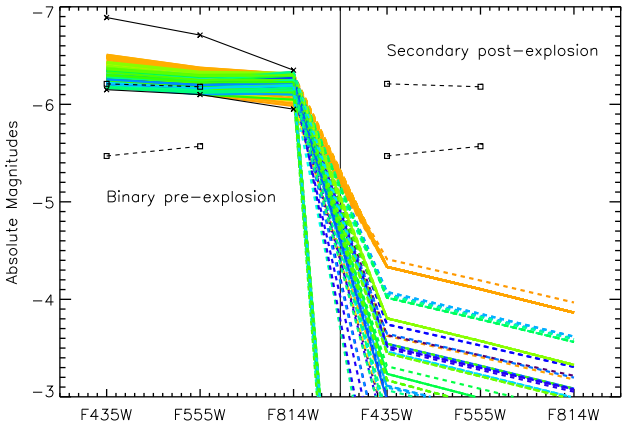

Figure 3. Spectral Energy Distributions of progenitor models compared to limits derived here with both the low- and high-extinction values used. The observed magnitudes have an error of ±0.3 mag. The left-hand panel shows the pre-explosion magnitudes for out models and the right-hand panel shows the post-explosion magnitudes. Pre-explosion observed magnitudes are shown in solid black lines, while the dashed lines represent the observed post-explosion magnitudes. Here, the colours of the lines represent the helium abundance of the model following the scheme used in Fig. 2.

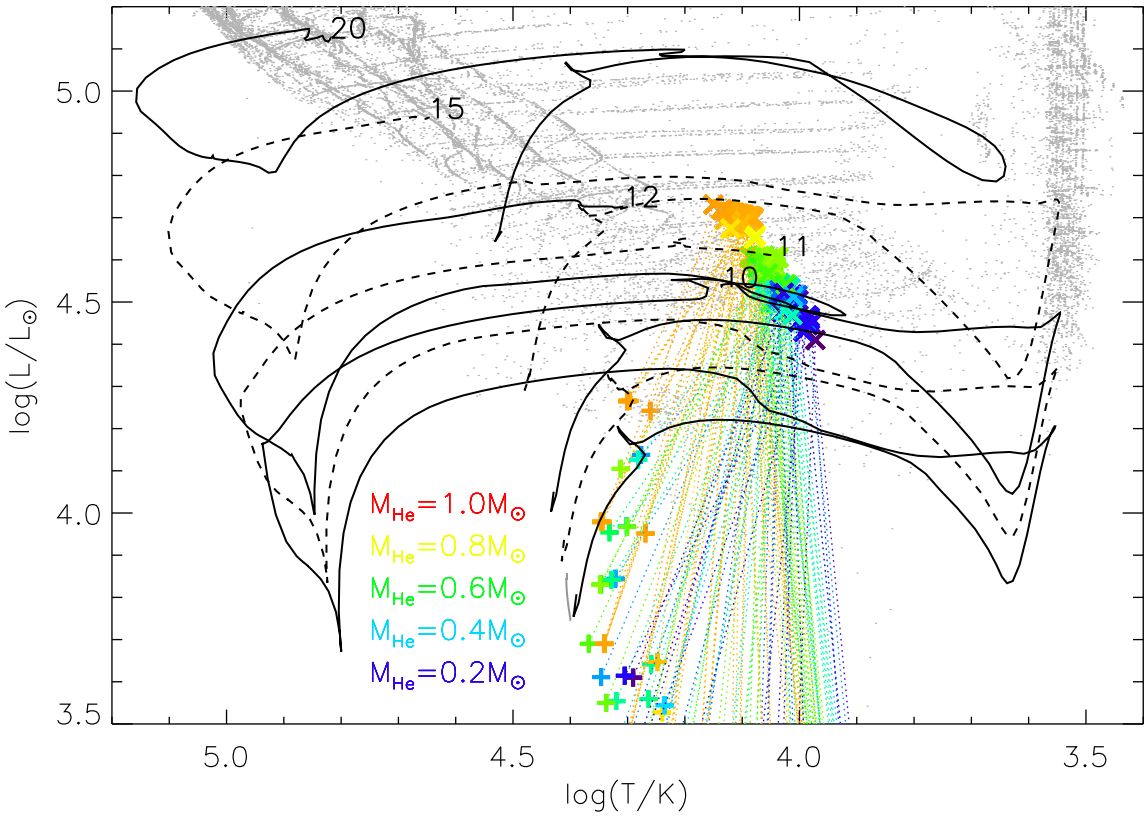

Figure 2. HR diagram showing the location of possible binary progenitor models (primary and companions) applicable to iPTF13bvn. The '×' show the location of the progenitor while the '+' is the companion. The colour indicates the mass of helium in the progenitor. The grey dots represent all possible progenitors of supernovae. The black solid and dashed lines are representative stellar evolution tracks for the primary star. The end point of each model is labelled with the stars' initial mass. The tracks are ordered in increasing initial mass of 10, 11, 12, 15 and 20 $M_\odot$.

Table 2. Physical parameters of the binary progenitor models which match the observed constraints on the progenitor of iPTF13bvn.

Primary parameter	Value	Secondary parameter	Value
$M_{1,i}/\mathrm{M}_\odot$	11.0 ± 1.2	$M_{2,i}/\mathrm{M}_\odot$	5.8 ± 2.9
$M_{1,f}\mathrm{M}_\odot$	2.4 ± 0.4	$M_{2,f}/\mathrm{M}_\odot$	5.0 ± 4.5
$\log(L_1/\mathrm{L}_\odot)$	4.6 ± 0.1	$\log(L_2/\mathrm{L}_\odot)$	1.1 ± 2.9
$\log(T_{1,\mathrm{eff}}/K)$	4.06 ± 0.04	$\log(T_{2,\mathrm{eff}}/K)$	4.0 ± 0.4
$\log(R_1/\mathrm{R}_\odot)$	1.71 ± 0.04	$\log(R_2/\mathrm{R}_\odot)$	0.4 ± 0.3
$M_{\mathrm{ejecta}}\,\mathrm{M}_\odot$	0.95 ± 0.4		
$M_{\mathrm{He}}\,\mathrm{M}_\odot$	0.6 ± 0.2		
System parameters			
$\log(P_i/\mathrm{d})$	1.9 ± 0.5	$\log(a_f/\mathrm{R}_\odot)$	1.8 ± 0.2
Age/Myr	24 ± 5	Z	0.027 ± 0.013

4 RESULTS AND DISCUSSION

Fig. 3 shows that in comparison to the similar diagram in Eldridge et al. (2015), the preferred progenitor is now a cooler helium giant, rather than a WR star. The main reason from this constraint can be understood in Fig. 3. The predicted pre-explosion magnitudes agree well with the observed magnitudes for low extinction, while all the predicted post-explosion magnitudes are at least 1 mag fainter than the late-time observed photometry. The more massive 17–20 $\mathrm{M}_\odot$ models from Eldridge et al. (2015) are ruled out because most of the pre-explosion magnitudes have a significant contribution from the companion star which would be brighter than the late-time magnitudes.

The mean parameters for the companion are shown in Table 2. The one value that is relatively unconstrained is the metallicity. While the mean metallicity is above Solar, we find fits to the progenitor between a mass fraction of $Z = 0.008$–0.040, or [O/H] = 8.5–9.2, the lower range of which is equivalent to that observed by Kuncarayakti et al. (2015). We note that the radius predicted from out models of $\sim$50 $\mathrm{R}_\odot$ is within the range allowed by the study of Bersten et al. (2014).

The secondary mass is also constrained to around 6 $\mathrm{M}_\odot$; however, the allowed range is quite large. We are able to rule out a star more massive than approximately 20 $\mathrm{M}_\odot$ via the late-time observations.

We show the evolution of an example system in Fig. 4. The hydrogen envelope is lost during a period of common-envelope evolution after the main sequence. We see little further mass is lost, otherwise, interior evolution progresses as it would with the hydrogen envelope (although the helium core does not experience dredge-up to reduce its mass).

An interesting prediction from our work is that in a sufficiently long observation, we might expect a late-time image of the SN location to reveal the companion as the SN should have faded below the possible companion magnitudes. For example, at 1000 d after explosion, the SN brightness would be of the order of $\sim$29.6 mag (as shown in Table 1), corresponding to an absolute magnitude of -2.1. The brightest companions we predict have an absolute magnitude of the order of -4, an apparent magnitude of 27.7. It is also possible, however, that a companion might be in the form of a black hole or neutron star, which would not be observable.

5 CONCLUSION

We have shown that the progenitor star of iPTF13bvn has disappeared and most likely had an initial mass between 10 and 12 $\mathrm{M}_\odot$ and had a companion star with a much lower mass; otherwise, it would have been observable in the post-explosion images. The mass range for the progenitor is a factor of 2 less than that suggested by Bersten et al. (2014); however, this was because they used the incorrect photometry of Cao et al. (2013). We note that they still suggest the progenitor was a helium giant although the final helium star mass is 3.5 $\mathrm{M}_\odot$.

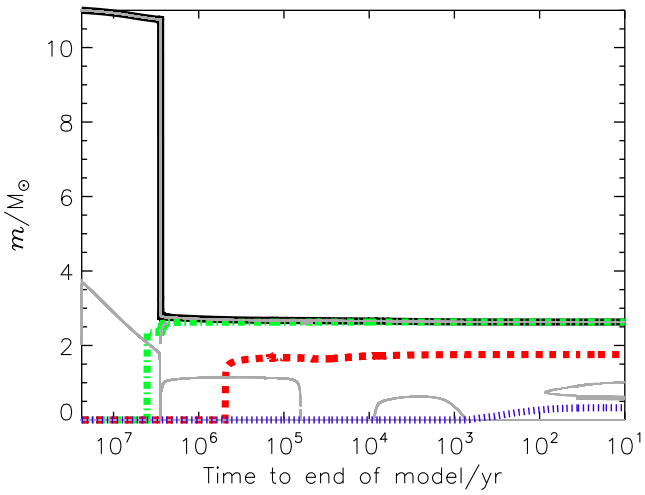

Figure 4. Kippenhahn diagram, for example progenitors of iPTF13bvn in the upper panel. The initial mass of the binaries stars were 11 and 5.5 $\mathrm{M}_\odot$ in an orbit with an initial period of 63 d. The thick black line represents the total stellar mass, the green dash–dotted line the mass of the helium core, the red dashed line the CO core mass, and the blue dotted line the ONe core. The thin grey lines represent the convective boundaries.

Our conclusions are strongly based on the caveat that the source seen in the late-time image is still the SN and not the companion star and that we can use the SN magnitude as an upper limit for the companion star.

We note that a recent similar deep search for the companion to SN 1994I, a Type Ic event, also did not find any progenitor (Van Dyk, de Mink & Zapartas 2016). This SN is considerably closer, so observations of the same depth reach lower absolute magnitudes of approximately -3.4 and derived a similar mass limit for the progenitor as we find here. In the case of iPTF13bvn, we have a firm constraint on the nature of the progenitor star and therefore the age of any companion star, this allows us to take account of the fact that stars become brighter and cooler as they evolve. In light of this, the limit on the mass of the companion to SN 1994I from Van Dyk et al. (2016) maybe be less than they found. Their study and our own however does begin to suggest that if the progenitor stars of Type Ib and Ic SNe are low-mass helium giants, the progenitors may be bright, their companions are also low mass and most likely faint and thus difficult to observe.

Another caveat is that these helium giants have still not been observed at any other time so their observable signature is uncertain as are the theoretical atmosphere spectra used to predict their brightness and colours. Here, the progenitor is too cool for using the Potsdam WR spectra, so we use the BaSeL spectra. The problem here is that those models are hydrogen rich. Kim, Yoon & Koo (2015) have calculated possible spectra using the detailed atmosphere modelling code CMFGEN; however, one problem is that these giants have low surface gravity which can significantly alter the shape of the spectrum. We confirm that we cannot fit any WR star models to the pre-explosion photometry, for iPTF13bvn, and still have a companion below the late-time magnitudes, whilst having an ejecta mass below 3 $\mathrm{M}_\odot$.

We also wish to make the community aware of the opportunity that there is now a better chance of detecting the companion star, as the SN should now have faded to the point where the companion should be directly detectable if a sufficiently long observation with *HST* was taken.

ACKNOWLEDGEMENTS

The authors thank the referee Christoffer Fremling for positive comments that greatly improved the Letter. JJE also thanks Morgan Fraser and Stephen Smartt for comments on an early draft of this Letter. JJE acknowledges support from the University of Auckland. The research of JRM is supported by a Royal Society Research Fellowship. The authors wish to acknowledge the contribution of the NeSI high-performance computing facilities and the staff at the Centre for eResearch at the University of Auckland. New Zealand national facilities are provided by the New Zealand eScience Infrastructure (NeSI) and funded jointly by NeSIs collaborator institutions and through the Ministry of Business, Innovation and Employments Infrastructure programme. URL: http://www.nesi.org.nz.nz.

REFERENCES

Alard C., 2000, A&AS, 144, 363
Alard C., Lupton R. H., 1998, ApJ, 503, 325
Bersten M. C. et al., 2014, AJ, 148, 68
Cao Y. et al., 2013, ApJ, 775, L7
Dolphin A. E., 2000, PASP, 112, 1383
Eldridge J. J., Izzard R. G., Tout C. A., 2008, MNRAS, 384, 1109
Eldridge J. J., Fraser M., Smartt S. J., Maund J. R., Crockett R. M., 2013, MNRAS, 436, 774
Eldridge J. J., Fraser M., Smartt S. J., Maund J. R., Crockett R. M., 2015, MNRAS, 446, 2689
Ergon M. et al., 2015, A&A, 580, 142
Folatelli G. et al., 2016, preprint (arXiv:1604.06821)
Fremling C. et al., 2014, A&A, 565, 114
Groh J. H., Georgy C., Ekström S., 2013, A&A, 558, L1
Kim H.-J., Yoon S.-C., Koo B.-C., 2015, ApJ, 809, 131K
Kuncarayakti H. et al., 2015, A&A, 579, 95
Srivastav S., Anupama G. C., Sahu D. K., 2014, MNRAS, 445, 1932
Stanway E. R., Eldridge J. J., Becker G. D., 2016, MNRAS, 456, 485S
Tully R. B. et al., 2013, AJ, 146, 86
Van Dyk S. D., de Mink S. E., Zapartas E., 2016, ApJ, 818, 75V
Wofford A. et al., 2016, MNRAS, 457, 4296
Yoon S.-C., Gräfener G., Vink J. S., Kozyreva A., Izzard R. G., 2012, A&A, 544, 11

This paper has been typeset from a TEX/LATEX file prepared by the author.